Learning Malware Representation based on Execution Sequences

Yi-Ting Huang, Ting-Yi Chen, Yeali S. Sun, and Meng Chang Chen

***Abstract*—Malware analysis has been extensively investigated as the number and types of malware has increased dramatically. However, most previous studies use end-to-end systems to detect whether a sample is malicious, or to identify its malware family. In this paper, we propose a neural network framework composed of an embedder, an encoder, and a filter to learn malware representations from characteristic execution sequences for malware family classification. The embedder uses BERT and Sent2Vec, state-of-the-art embedding modules, to capture relations within a single API call and among consecutive API calls in an execution trace. The encoder comprises gated recurrent units (GRU) to preserve the ordinal position of API calls and a self-attention mechanism for comparing intra-relations among different positions of API calls. The filter identifies representative API calls to build the malware representation. We conduct broad experiments to determine the influence of individual framework components. The results show that the proposed framework outperforms the baselines, and also demonstrates that considering Sent2Vec to learn complete API call embeddings and GRU to explicitly preserve ordinal information yields more information and thus significant improvements. Also, the proposed approach effectively classifies new malicious execution traces on the basis of similarities with previously collected families.**

***Index Terms*—deep learning, malware analysis, malware family classification, neural network**

I. Introduction

Malware such as computer viruses, Internet worms, and Trojan horses is one of the main threats in computer security, because with it malignant actors disrupt or infect network services, destroy software or data, steal sensitive information, or take control of a host, often resulting in personal or business losses. This explains the growing interest in malware detection [1], [2], [3], [4], [5], [6], [7], [8] and malware classification [9], [10], [11], [12], [13], [14].

Anti-virus products have focused on using individual malware signatures to detect malware. More recently, with the development of obfuscation techniques, a number of variants of a malware family can be mutated using polymorphic or metamorphic techniques. As the resultant similar behavior increases the difficulty of identifying effective signatures, malware can bypass static signature-based detection and evade commercial virus scanners [4], [15]. In addition, both Sebastián [16] and Chiu [17] pointed out that labels from different anti-virus vendors are inconsistent. Thus malware may have different family labels assigned by different AV vendors. This can be a limitation for a model which assigns only one label to each malware sample.

When investigating a given malware sample, most current studies propose end-to-end systems to detect whether the sample is malicious or to identify its malware family. However, from Chiu's [17] observation, variants from the same family can exhibit distinct behavior. If a model analyzes malware only as a single unit, it can fail to detect or classify unseen variants of known malware. Thus, rather than detecting individual malware signatures, a number of studies [11], [12], [13], [17], [18] focus their attention instead on analyzing malware behavior recorded at runtime.

Instead of considering a malware sample as a whole, we consider if malware has common behaviors inherited from its malware family. The grouping criteria of a malware family are based on common characteristics such as attribution to the same authors or the same intention, which reflect the main intents from the observed execution activities. Fig. 1 describes our intuition. Malware samples within the same family share characteristics from execution traces. We design a neural network framework to capture this invariant representation within a family, which should exclude distinct behaviors. Moreover, when an unknown sample is given, its representation can be compared with the learned common characteristics of families. Sufficient matches can identify the sample as belonging to a known malware family.

In this paper, we classify neural malware families by learning malware representations. A malware representation is learned using an embedder, an encoder, and a filter. The embedder is composed of two state-of-the-art embedding models — BERT [19] and Sent2Vec [20] — to capture relations within a single API call and among consecutive API calls in a trace. The encoder comprises two neural layers: a gated recurrent unit [21] designed to preserve the ordinal position of API calls in the trace, and a self-attention mechanism [22] to compare intra-relations among the different positions of API calls. The filter

This work was supported in part by MOST 108-2218-E-002-045, MOST 107-221-E-002-002-MY2, and Research Center for Information Technology Innovation, Academia Sinica.

Yi-Ting Huang is with the Institute of Information Science of Academia Sinica, Taipei, Taiwan (e-mail: ythuang@iis.sinica.edu.tw).

Ting-Yi Chen was with the Department of Information Management of National Taiwan University (e-mail: r06725035@g.ntu.edu.tw).

Yeali S. Sun is with the Department of Information Management of National Taiwan University (e-mail: sunny@ntu.edu.tw).

Meng Chang Chen is with the Institute of Information Science of Academia Sinica, Taipei, Taiwan (e-mail: mcc@iis.sinica.edu.tw).

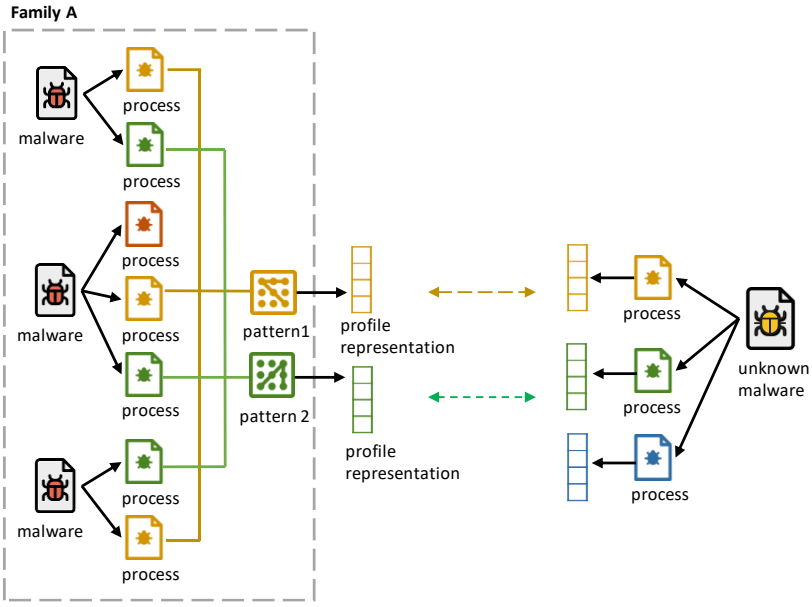

Fig. 1 Proposed framework. The model learns malware representations from common patterns within a family. When given an unknown sample, the proposed model finds the most similar characteristics from a known family.

identifies representative API calls to build a malware representation for family classification. The model corrects shortcomings of previous work, which pay attention only to a single malware sample's behavior without accounting for common characteristics within a family. In general, the proposed framework leads to a better understanding of malware characteristics for malware family classification. This paper makes the following contributions:

- We develop a neural network framework to learn malware representation based on invariant characteristics of a malware family.
- We design an embedder to preserve semantics of parameters in API statements from a malware execution trace.
- We design an encoder that takes into account temporal relationships and correlates relevant events of API statements in a malware execution trace.
- We visualize malware representation in a temporal space, demonstrating that the representation is explainable with physical meaning.

II. Related Work

A. Features Used in Static and Dynamic Analysis

A large body of literature exists in malware behavior analysis. This can be classified into static analysis [2], [23] and dynamic analysis [11], [12], [13], [18].

Static analysis collects information from binaries or source code by decompressing or unpacking rather than executing them. Input features such as byte sequence n-grams [3], [5], opcodes [24], [25], string signatures [6], and control flow graphs [26] are used in static analysis. Saxe et al. [5], an example of static analysis, incorporated features extracted from binary PE files such as contextual bytes, PE imports, string 2d histograms, and PE metadata features into a deep neural network model. They demonstrated low false positive rates and high scalability. Malware derived from the same source code or belonging to the same family often shares a large percentage of source code or instruction blocks; however, this approach does not work for obfuscated malware.

Dynamic analysis focuses on execution activities from Windows API calls [11], [13] or system calls [24] when a device has been infected. Activities such as registry calls, file I/O, and network features are used to identify malicious activity. Dahl et al. [11] extracted patterns observed from tri-grams of system API calls, distinct combinations of a single system API call and an input parameter identify a file as malicious or benign. DeepSign [13] selected frequent unigrams of Windows API calls from a log file generated by Cuckoo sandbox and transformed these into binary vectors to train a deep belief network for classifying malware and benign files. Dynamic analysis not only accounts for obfuscated, encrypted, and packed source code, but also captures malicious activities from observed evidence.

B. Machine Learning and Deep Learning for Malware Analysis

Over the last few decades, there has been a dramatic increase in the number of publications on malware analysis using machine learning techniques. Algorithms such as naive bayes [1], decision trees [27], [28], support vector machines [27], [28], and random forests [28] have been investigated for malware detection. These have shown that behavior patterns obtained from statistical methods can be used to detect or classify unknown samples into their families successfully; the methods yield comparable performance.

In recent years, we have seen mounting evidence of the

usefulness of incorporating neural networks into malware analysis; this produce better results than using machine learning techniques. Dahl et al. [11] trained an artificial neural network model for malware detection. Athiwaratkun et al. [14] treated an API call event as a character, and applied convolutional neural networks to learn character-based events for malware classification. Agrawal et al. [7] combine two powerful neural network models—long short-term memory (LSTM) networks and convolutional neural networks (CNNs)—for malware detection. Agrawal et al. [8] presented attention-based recurrent neural networks for capturing local event patterns in ransomware sequences. At present, however, most current malware analysis systems focus on end-to-end neural network models to detect whether a sample is malware, or identify which malware family it belongs to, without interpreting the sample in a physical numerical space.

III. Malware Execution Profile and Representative Motif Sequence Generation

When given a malware sample, we first use an automatic dynamic malware profiling system to record execution profiles as inputs, after which profiles in the same families are aligned and grouped using the runtime API call sequence-based motif mining algorithm (RasMMA) [17], a clustering algorithm which extracts common behaviors within a family as outputs.

A. Execution Trace Generation

1) VMI-based profiling system

To capture the essentials of the execution behavior of a malware program and to enable the target system to identify and characterize the intent of every phase's operations during the course of the execution of the malware, we use an automated dynamic malware behavior profiling and analysis system based on virtual machine introspection (VMI) [29], [30]. This system hooks 62 carefully-selected Windows API calls in five categories: library use, process invocation, file I/O, registry access, and network access. Unlike many past dynamic behavior analysis system or tools, which record only API function names for profiling, the system additionally records parameters and return values, for example allowing users to understand what process is opened or what DLL file is loaded. Moreover, since in the Windows system, the registry contains important configuration information for the operating system, services, applications, and user settings, registry-related operations are important in malicious behavior analysis; parameter values are particularly critical. For instance, *RegQueryValue()* is called by many programs to check system or application settings. Given the registry key path and value name for the function's *hkey* parameter, we can determine which registry the query refers to. In the profiling system, the function name and its corresponding parameter values and return value are all recorded. Also, a malware sample may create or fork one or more processes. One execution trace is generated per process. The advantage of the system is that it records only selected API calls rather than all system calls, which reduces trace sizes by at least two orders of magnitude.

2) Trace cleaning

Recording five minutes of Windows API calls yields voluminous information. Shown in TABLE I are the 26 selected API function names, along with their associated parameter types and return values. As some malware duplicates the same API call repeatedly, in our recorded execution profile only the first API call is retained. For instance, a library file is reloaded by *LoadLibrary()* repeatedly; thus only the first API call is retained after cleaning the trace.

TABLE I
SELECTED WINDOWS API FUNCTION NAMES AND PARAMETER TYPES

Category	API function name	Parameter name
Registry	RegCreateKey, RegDeleteKey, RegDeleteValue, RegEnumValue, RegQueryValue, RegSetValue	hKey, lpSubKey, lpValueName
Process	CreateProcess, CreateRemoteThread, CreateThread, TerminateProcess, ExitProcess, OpenProcess, WinExec	lpApplicationName, dwCreationFlags, uExitCode
Network	nternetOpen, InternetConnect, HttpSendRequest, GetUrlCacheEntryInfo, WinHttpConnect, WinHttpOpen, WinHttpOpenRequest, WinHttpReadData, WinHttpSendRequest	lpszServerName, pswzServerName, nServerPort
Library	LoadLibrary	lpFileName
File	CopyFile, CreateFile, DeleteFile	lpFileName, lpExistingFileName, lpNewFileName, dwCreationDisposition, dwDesiredAccess, dwShareMode

3) Parameter winnowing

An execution trace contains all the parameter values of hooked API calls. We consider that not all parameter values directly reflect the semantics of the operation, and that malware with the same intent can have slightly different parameter values such as user-profile folders "*user's Desktop*" and "*user's Documents*", depending on the version of operating systems or its executable strategy. Thus parameter values are symbolized to select only significant parameters of an API call and reduce noise as described in [17]. Also, the traces are reformatted to present a Windows API call line by line.

B. RasMMA

RasMMA (runtime API call sequence-based motif mining algorithm) [17] extracts common behaviors from a group of malware. Given two distinct clusters, an alignment of the two API call sequences is obtained via global sequence alignment (GSA) [31]. Similarity scores are then computed and ranked to determine whether the clusters should be merged or a new cluster created. This process is iterated until the termination conditions are met, resulting in not only the sequence motifs among the sequences, but also a set of behavior trees in the

given set. A behavior tree is comprised of profiles having the common motifs. An example is shown in Fig. 2. Leaves G1, G2, G3, and G4 represent profiles and behavior trees G6 and G5 represent common motifs among the children. Note that G4 is judged to be a loner tree because it has no sequences in common with the other given profiles.

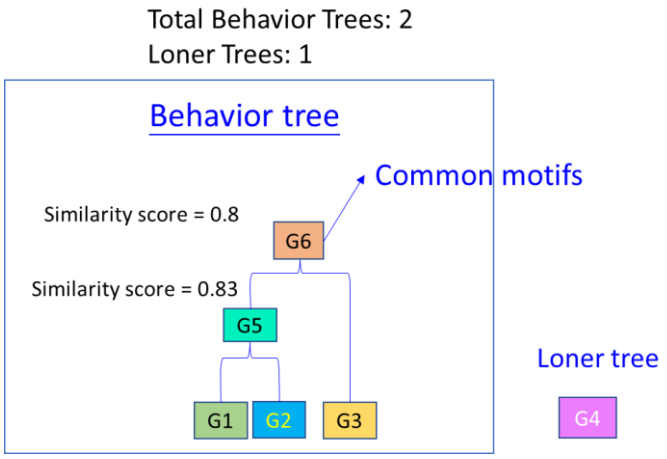

Fig. 2. Output from RasMMA: two behavior trees and a loner tree

IV. Profile Representation

The purpose of this study is to build a profile representation by identifying a representative motif sequence from a given execution profile. The three proposed modules include (a) an embedder to transform each Windows API call invocation into a numerical vector and preserve relations within API call invocations and semantics of parameter values, (b) an encoder to process sequences of Windows API call vectors and calculate the associations among them, and (c) a filter to examine the importance of each Windows API call invocation and present the predicted representative motif sequences as a profile representation. Fig. 3 describes the model architecture.

A. Task Definition

Given an input trace $\boldsymbol{x}$, we seek to identify the importance $\boldsymbol{b}$ of each Windows API call invocation to form a profile representation $\boldsymbol{r}$. Given m Windows API call invocations, $\boldsymbol{x}$ is represented as $\boldsymbol{x} = \{x_1, \ldots, x_m\}$. The corresponding prediction $\boldsymbol{b} = \{b_1, \ldots, b_m\}$ is a series of binary variables denoting whether call invocation x_i is representative.

B. Embedder

A profile consists of a number of Windows API calls, each of which includes one or more parameter values, but with an enormous and diverse range of values. Complicating analysis, some malware generates random variables as parameter values. For example, *Backdoor:Win32/Simda* copies itself as "*<variable><number>.exe*" and generates various URL addresses to confuse anti-virus programs. The resulting unpredictable and sparse parameter values thus preclude the use of traditional methods such as term frequency.

An embedder takes a variable-length execution trace $x = \{x_1, \ldots, x_m\}$ as the input and outputs a sequence of embedding vectors $x' = \{x'_1, \ldots, x'_m\}$. A Windows API invocation call x_i consists of an API function name n_i, one or more parameter values p_i, and one (if any) return value ret_i. Previous work used one-hot encodings [7] or a learnable embedding matrix [8], [32] to represent input embeddings. Since parameter and return values are also considered in this work, it is difficult to adopt these approaches directly because of the infinite number of values. Additionally, advances in transfer learning such as ImageNet [33] first pre-train a neural network on a task and then fine-tune it to yield a new purpose-specific model. Thus, the embedder uses two state-of-the-art pre-trained models — BERT [19] and Sent2Vec [20] — to build an embedding matrix.

BERT (bidirectional encoder representations from transformers) [19] is used to initialize the function name embedding n'_i. It yields promising results in natural language processing tasks such as natural language processing and question answering. The key innovation of BERT is the learning of contextual relations not only between tokens in a single sentence but also between two contiguous sentences. BERT is pre-trained on Wikipedia articles and BooksCorpus and has been publicly released[1].

The trained BERT model is used as the basis for our embedder and is fine-tuned[2] on our dataset. This allows the embedder to enhance the structure of a single Windows API call, including a function name, one or more parameter values, and one (if any) return value. Moreover, it yields a better understanding of relationships between two Windows API calls. Here, we take a single profile as a document and a single Windows API call as a sentence. After the training, we extract the last four hidden states of the selected function names and average them to initialize the learnable embedding matrix E as

$$n'_i = En_i \tag{1}$$

where a parameter matrix $E \in R^{d \times |n|}$, where $|n|$ denotes the number of selected function names, $n = 26$, and d denotes the embedding size, $d = 768$.

Sent2Vec [20], used here for the complete Windows API call embedding c'_i, is an unsupervised learning model for sentence embeddings, the basic concept behind which is that it considers not only unigrams but also n-gram sequences in a single sentence, allowing the model to learn the sentence embedding based on its possible constituent words.

We treat a Windows API call as a sentence and use Sent2Vec to learn universal API call invocation embeddings. First, a complete Windows API call invocation x is changed to lowercase and tokenized by the delimiters ". ; , - + ^ ( ) / @ # ? ! & $: } { \ * % ~ ' " = _ ". The model learns each token and n-gram embedding shown in a single Windows API call invocation. The complete API call embedding c'_i is then the average of the n-gram embeddings along with the words

[1] https://github.com/google-research/bert

[2] https://github.com/huggingface/pytorch-transformers/tree/master/examples/lm_finetuning

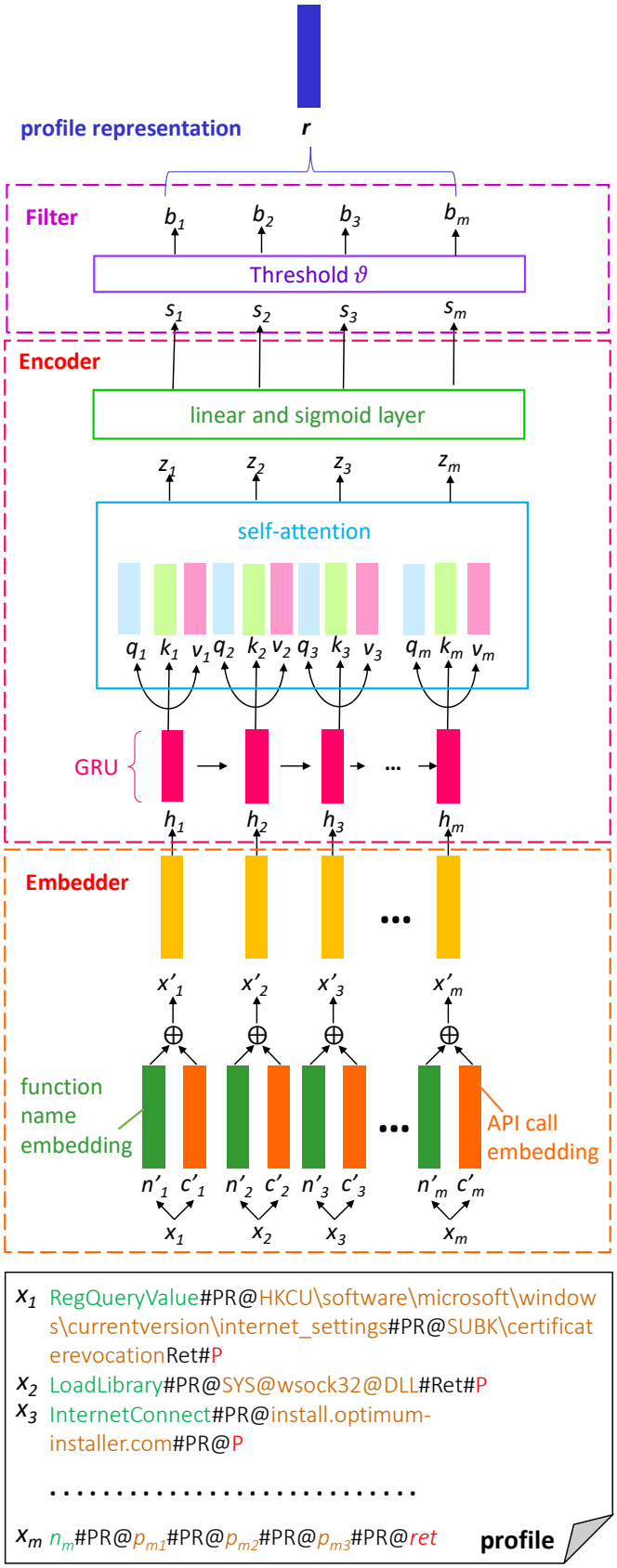

Fig. 3. Model architecture

$$c_i' = Sent2Vec(x_i) = \frac{1}{|R(x)|}\sum_{w \in R(x)} c'_w \quad (2)$$

where $R(x)$ is the list of n-grams in a given Windows API call invocation x, $c' \in R^{d \times 1}$ represents the learned source embedding, and d denotes the size of embedding size, d = 768. The embedding matrix $\boldsymbol{C}' \in R^{d \times |c|}$ is obtained after training on our dataset and is frozen in the following procedure, where $|c|$ denotes the number of API calls in our dataset.

Each embedding x'_i is composed of a function name embedding n'_i and a complete API call embedding c'_i:

$$x_i' = n_i' \oplus c_i' \quad (3)$$

where $\oplus$ is element-wise addition. The function name embedding and complete API call embedding, projected to d-dimension numerical space respectively, are summed to represent a Windows API call.

C. Encoder

An execution profile may be comprised of sequences of normal behavior, a number of redundant events, and a sequence of malicious actions. This can complicate the identification of representative motif sequences. Also, mixed dependencies exist among a sequence of Windows API call invocations. Therefore, it is crucial to recognize essential patterns in a given execution profile.

With the encoder, we seek to process each API call invocation embedding $x' = \{x'_1, \ldots, x'_m\}$ in an execution profile and produce a series of importance scores $s = \{s_1, \ldots, s_m\}$. A given trace contains an arbitrary number of API call invocations, each of which may have close dependencies. The encoder accounts for this using a GRU layer, a self-attention layer, and a sigmoid layer. The GRU layer processes the time-series information over input embeddings, the self-attention layer calculates the association between input embeddings, and the sigmoid layer outputs a ratio between the probability that a certain API call is important or not.

Gated recurrent units [21] are part of the recurrent neural network (RNN) family and are used to learn a hidden state h_i at timestep i which can be seen as a summary of the past sequence from the beginning up to i-1 and the current input x'_i.

$$h_i = GRU(x_i', h_{i-1}) \quad (4)$$

This summary maps an arbitrary length sequence $\{h_1, \ldots, h_{i-1}\}$ and the current observation x'_i to a fixed length vector h_i. It preserves the ordinal position of the API calls in the trace. That is, the GRU hidden state h_i at time i is indeed the result of processing the API call embeddings from the first x'_1 to the current observed API call embedding x'_i. Moreover, compared to other RNNs, GRU not only solves the vanishing gradient problem [34] but also produces equally excellent results.

We utilize a self-attention layer [22] to compute the weighted API call representation Z over the output H from the GRU layer. The hidden matrix H from GRU is projected into distinct key, value, and query representations K, V, and Q with three distinct

weight matrices W^K, W^V, and W^Q respectively, where $K, V, Q \in R^{m\times|h|}, W^K, W^V, W^Q \in R^{|h|\times|h|}$. The attention weights are calculated by comparing each pair of Windows API calls from Q and K, scaled by the inverse square root of their hidden dimension $|h|$, and normalized with the softmax function to produce a distinct distribution for each API in a profile. Finally, these weights are then multiplied by themselves V to obtain the self-attended API call representations

$$Z = softmax(\frac{QK^T}{\sqrt{|h|}})V, \quad (5)$$

where $Z \in R^{m\times|h|}$.

A self-attended API call representation z_i can be seen as the weighted summarization with respect to the API call input i over the API call representations in V. This is in contrast to previous work [32] which focuses only on consecutive API call sequences in a given profile. The self-attention mechanism compares intra-relations and captures the relative importance among the different positions of API calls. This helps the model learn relative information from inconsecutive API calls.

Representation Z is then passed to a feed-forward layer, which consists of a linear layer and a sigmoid layer. The sigmoid layer outputs the conditional probabilities of the estimation, called importance score $s = \{s_1, \ldots, s_m\}$. It describes the ratio between the probability that a Windows API call is important, and the probability that it is not:

$$S = sigmoid(ZW^z), \quad (6)$$

where $W^z \in R^{|h|\times 1}$.

D. Training

We trained the model using binary cross-entropy loss:

$$L = -\frac{1}{n}\sum_{i=1}^{n} s_i \log(\hat{s_i}) + (1 - s_i)\log(1 - \hat{s_i}), \quad (7)$$

where n is the number of profiles in a training set. The Adam optimizer [33] was used, and early stopping [35] was employed on the development set to prevent overfitting.

E. Filter

Once the model is well-trained, the filter is a threshold by which to examine each value of the predicted importance score $\hat{s} = \{\hat{s_1}, \ldots, \hat{s_m}\}$ on the development set and transform it into a series of binary vectors $b = \{b_1, \ldots, b_m\}$ if it does not meet the boundary condition ϑ. Here, $b \in \{0,1\}$ and $0.01 \leq \vartheta \leq 0.99$.

$$\vartheta = argmin_\vartheta\, Fscore(s, b) - hammingloss(s, b) \quad (8)$$

The threshold is selected based on the difference between the F1 score and Hamming loss. F1 is the harmonic average of the precision and recall, and Hamming loss is the fraction of the wrong labels to the total number of predictions. Thus, the threshold is chosen where the performance is best with the fewest mislabels. Threshold value ϑ is selected on the development set, as described in Section V.D.

F. Profile representation

The profile representation r is the mean of the selected Windows API call embedding x' corresponding to the estimated binary vector b.

$$r_i = \frac{\sum_{i=1}^{m} b_i x_i'}{\sum_{i=1}^{m} b_i} \quad (9)$$

V. Performance Evaluation

A. Dataset

We collected 24,096 malware samples. Using the VMI profiling system, we recorded 33,496 profiles from 21,724 samples. 2,372 samples failed because they were not executable files.

To obtain the family labels for our samples, the samples were uploaded to the VirusTotal website[3] in May, 2019. VirusTotal returned more than 50 family labels defined by various anti-virus vendors. However, the family labels have some differences. For example, *000e99026fee09d3bf5f51f9a6fcc9543cbe9088d60c84 4afb10c38d69f3b91d*, is labeled *WORM/Vobfus.CF*, *Gen:Variant.Chinky*, and *Win32/AutoRun.VB.AGQ*, by Avira, BitDefender, and ESET-NOD32 respectively. Anti-virus vendors each have their own naming schemes, and thus seldom reach a consensus. In previous work [17], we describe how we determined the family label for each sample in our dataset.

First, we filtered out anti-virus vendors with low detection rates and benign samples. We selected as our representative anti-virus vendors those 47 anti-virus vendors which returned more than 40% of the detection results in our dataset. We removed 158 samples which were not detected as malicious by the anti-virus vendors. Second, we removed irrelevant strings in the collected labels. Each label was changed to lowercase and tokenized by delimiters "\ , ! ( ) [ ] @ : / . _ - ". Tokens in a generic list[4] or tokens whose length is less than three were removed, except for *kdz*, *ipz*, and *lmn*. Third, the family label was decided by a majority vote. To ensure labels were consistent with most of the representative anti-virus vendors, we kept samples for which 10% of the vendors assign the same family name; in this step we excluded 6,072 samples. The majority result among anti-virus vendors was used as the

[3] https://www.virustotal.com

[4] Collected manually, the generic list includes adinstaller, adware, agent, antifw, antifwk, appl, application, applicunwnt, autorun, backdoor, behaveslike, bundleapp, bundler, bundleinstaller, click, cloud, crypt, cryptor, confidence, deepscan, der, dropped, dropper, downloader, downware, eldorado, famvt, generic, grayware, hacktool, heur, heuristic, high, hw32, in-trojan, inject, injector, install, installer, kcloud, malicious, malware, malware-cryptor, monitoringtool, networm, not-a-virus, oscope, optional, p2p-worm, packed, patcher, psudocode_V2.0.txt, potentially, wriskware, software, suspicious, tool, toolbar, troj, trojan, trojandownload, trojware, trojan-downloader, trojan-dropper, trojan-clicker, unknown, unwanted-program, variant, virus, win32, worm, and xpack.

sample's family label. Finally, to assure that patterns from a family were representative, we removed families with less than fifteen samples, yielding 168 families.

RasMMA was executed to produce the gold importance scores *s*. Taking *0.8* as the RasMMA similarity threshold, 4,877 profiles were treated as loners and excluded as they showed no common behavior with others. Loner profiles will be discussed in Section VII. As two families showed no common behavior patterns, 23 samples from both families were removed. Lastly, we eliminated 4,877 profiles: those that belonged to fewer than three behavior trees or that contained fewer than ten motifs. This resulted in 9,819 profiles from 6,585 samples and 135 families yielding 1,041 behavior trees.

Since in practice some profiles contained too many or too few API calls, we excluded those samples with more than 226 API calls (8%). The final dataset included 8,176 profiles from 6,056 samples, 133 families, and 808 behavior trees. The details are shown in TABLE II.

TABLE II
DESCRIPTIVE STATISTICS

		Samples	Profiles	Family	BT
Original		24,096	-	-	-
After	VMI profiling	21,724	33,496	-	-
	Family voting	13,903	21,774	168	-
	RasMMA labeling	6,585	9,819	135	1,041
	Length pruning	6,056	8,176	133	808

We randomly divided the dataset into a training set (80%), a development set (10%), and a testing set (10%). If a sample had fewer than 10 behavior trees, it was excluded from the development and test sets. More details are shown in TABLE III.

TABLE III
DESCRIPTIVE STATISTICS FOR TRAINING, DEVELOPMENT, AND TESTING SETS

	Training set	Development set	Test set
Samples	5,466	431	481
Profiles	7,215	453	508
Families	133	47	47
Trees	808	135	135

B. Implementation Details

We set the embedding unit and the hidden unit size to 768 and 192 respectively. We used the Adam optimizer with a learning rate of 0.001. We trained for 119 epochs; the best model was selected at the 89th epoch based on the lowest validation loss, as shown in Fig. 4. The mini-batch size for the update was set to 128, and threshold ϑ was selected as 0.51 based on the development set.

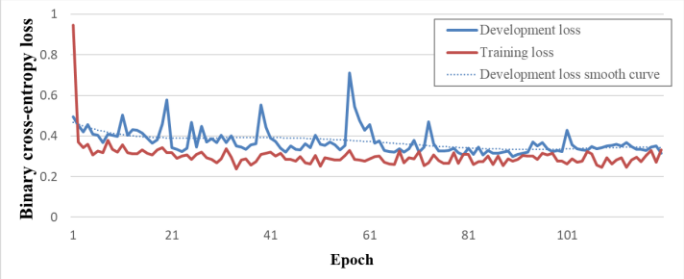

Fig. 4. Training and development set loss

C. Metrics

To compare the estimated binary vector *b* with the gold important score *s*, we report our result on the test set with the following evaluation criteria:

- True positive (TP): prediction $b = 1$ and gold score $s = 1$
- False positive (FP): $b = 1$ but $s = 0$
- False negative (FN): $b = 0$ but $s = 1$
- Precision denotes the number of estimated important Windows API calls that are predicted correctly: $P = \frac{TP}{TP+FP}$
- Recall denotes the ratio of correctly estimated important Windows API calls to all profiles, reflecting the classifier's ability to detect all important API calls: $R = \frac{TP}{TP+FN}$
- The F1 score denotes the weighted average of precision and recall: $F = \frac{2PR}{P+R}$
- Hamming loss denotes the fraction of mislabeled labels to the total profiles (Schapire and Singer, 1999): $H = \frac{XOR(b,s)}{m}$, where *m* is the number of API calls in a given profile.

D. Effectiveness of each component in the framework

We conducted ablation tests to assess the impact of

- Using both the function name embedding and the complete API call embedding for the input embedding;
- Using both the GRU and self-attention for the encoder.

For the encoder, we additionally used two baseline components: a multi-layer perceptron (MLP) and a Transformer encoder [22]. The MLP is a traditional neural network in which we use two fully connected layers without any recurrent neural units or attention mechanism. The Transformer encoder is composed of positional encoding, self-attention, and a multi-head attention mechanism. It adds positional information with the numbers between [-1, 1] using a predetermined sinusoidal function to the input embeddings, rather than the learned GRU.

TABLE IV shows the performance for each model. The proposed model outperforms the other models by a large margin, showing that the proposed components in both the embedder and the encoder facilitate representative API call detection. The model clearly improves significantly when considering complete API call embeddings, demonstrating that the parameter values and the return values of a Windows API call explicitly provide more information and make it easier for the neural model to learn input values in a latent way. In addition,

the performance drops when the encoder is replaced with the Transformer encoder with position encoding, suggesting that the learned GRU plays an important role in preserving ordinal information within Windows API calls.

TABLE IV
EXPERIMENTAL RESULTS

	P	R	F1	H
Proposed framework	**0.882**	**0.866**	**0.874**	**0.045**
Embedding				
w/o function name embedding	0.858	0.860	0.859	0.051
w/o API call embedding	0.710	0.851	0.774	0.089
Encoder				
MLP	0.639	0.731	0.682	0.122
Transformer encoder (2017)	0.475	0.506	0.490	0.189
w/o self-attention	0.780	0.400	0.529	0.128

To better understand the effect of filter thresholds, we evaluated the proposed framework with thresholds from 0.01 to 0.99 on the test set. Fig. 5 is a plot of the test set performance in terms of four metrics. We observe that values in binary vectors are not filtered out for low thresholds, resulting in high recall but low precision from 0.01 to 0.49. At a threshold of 0.49, however, precision increases and Hamming loss falls, both dramatically. The best threshold on the development and test sets is 0.51. Thus, the leveraged strengths of both F1 and Hamming loss result in better overall performance.

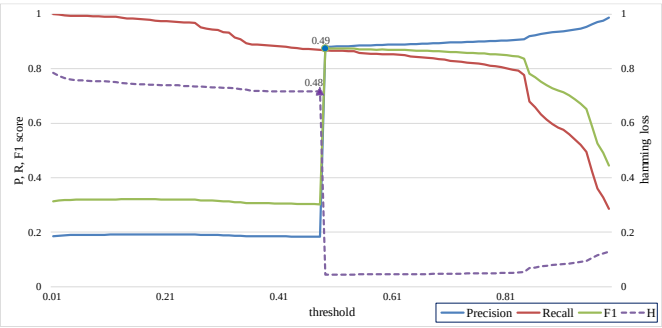

Fig. 5. Experimental results on different thresholds in the filter setting

VI. MALWARE FAMILY CLASSIFICATION EVALUATION

A. Experimental Setting

Using the same dataset from Section V.A and given a profile representation r from the test set, we computed the cosine similarity between the profile r and each profile r_t in the training set.

$$p = argmax_t\ sim(r, r_t) \tag{7}$$

The estimated family label $\hat{f}_r$ is assigned based on the family label f_p for the most similar profile p in the training set. Note that when more than one profile in the training set has the same (largest) similarity value, we consider all such family labels to be the predicted labels.

[5] http://projector.tensorflow.org/

B. Results

The proposed model predicted API calls deemed representative based on the family characteristics; however, no API calls in 125 profiles (33%) in 22 families were predicted as "representative". One reason is the trade-off between recall and precision discussed in Section V.D. Another possible reason is there was less training data for these 22 families than for other families. For example, as *Sirefef* had only 10 profiles in the training dataset, it was difficult to learn its profile representations.

In general, 374 to 508 profiles were correctly classified. Of the 383 estimated profiles, 97.65% were correctly matched to their own family. In particular, the profiles from thirty-nine families were 100% correctly estimated, suggesting that profile representations estimated by the proposed framework are robust across most malware families.

Fig. 6 shows the match/mismatch results from the profiles in the seven families. In most cases, when a profile's family is estimated incorrectly, its behavior tree is also assigned incorrectly. The sole exception is a profile from the *vilsel* family, which shares a behavior tree with another malware family.

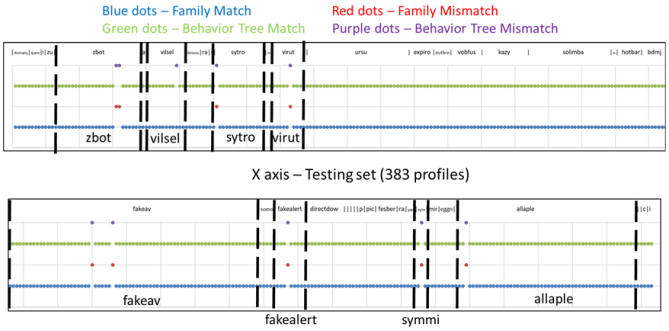

Fig. 6. Match/mismatch results for seven families

VII. DISCUSSION

In this section, we visualize profile representations for the *Allaple* malware family to investigate the meanings of profile representations and loner trees in a given family, and to compare with profile representations from other families.

We extracted each *Allaple* profile representation in the training set and test set respectively, and transformed them into 2-dimensional vectors using an embedding projector [5] with UMAP [36]. The four major groups, corresponding to four RasMMA behavior trees, are shown in Fig. 7. Results show that most test set profiles are located near those from the training set. In TABLE V we provide a semantic description of each group: the model seems to learn the hidden information behind the behavior tree in both numerical and semantic spaces.

The profiles, from *Allaple* but excluded in our dataset, were vectorized by the proposed model and visualized in Fig. 8. Although the samples were assigned the same labels by anti-virus vendors, they are loners because their characteristics differ greatly from the others in the same family. Results show that the loners are not located near the dominant groups from

the training set. This supports the results from [17], that is, the behavior of loners is distinct from those in the same family, and samples categorized by family names can be inconsistent even though they are decided by the majority.

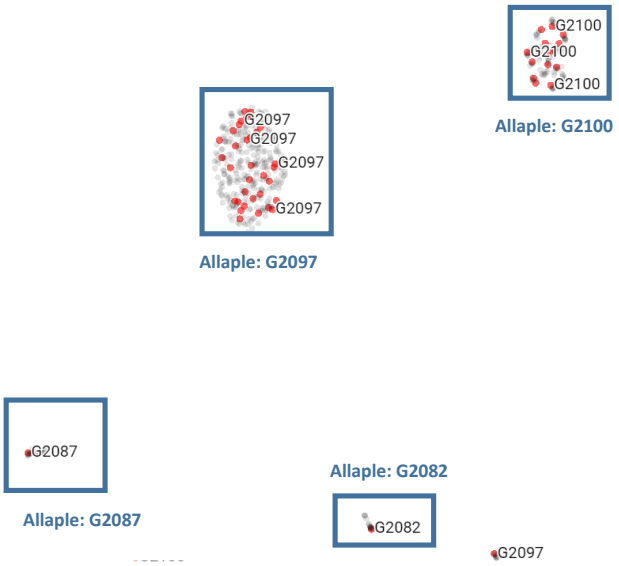

Fig. 7. 2D embedding of profile representations from *Allaple* family. The points (gray from training set, red from test set) are grouped by behavior trees.

TABLE V
SEMANTIC DESCRIPTION OF FOUR CLUSTERS

ID	Semantic description of behavior tree
G2097	Queries registry about *winsock2* and accesses crypt32.dll library.
G2100	Queries registry about *winsock2*.
G2087	Queries OS version and any information about installed browser.
G2082	Malware repeatedly reduplicates itself as crack game executable file or program password generator.

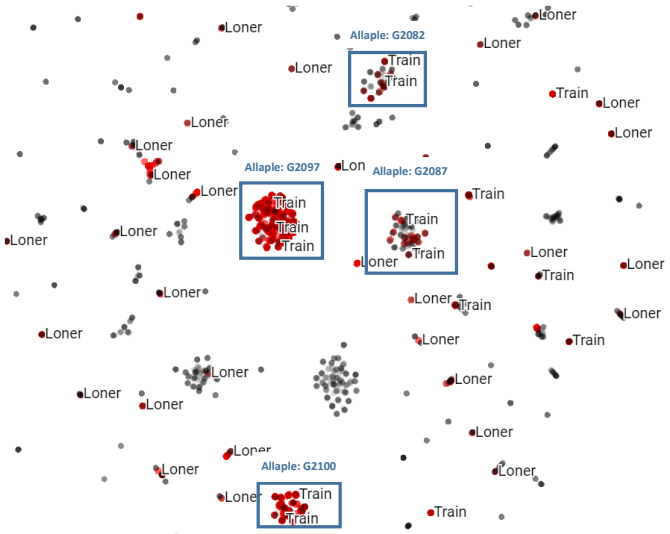

Fig. 8. 2D embedding of loner profile representations in *Allaple* family

Fig. 9 shows all profile representations in the training set. Many profiles in the different families overlap within the major four behavior groups in the *Allaple* family. Our assumption is that families are differentiated from each other by behavior trees; however, this finding does not support this assumption. This could be due to pluralism, that is, the characteristics of a behavior tree extend across more than one family. For example, the *graftor*, *virut*, and *exiro* families share the G2097 behavior tree; *symmi*, *solimba*, and *zusy* share G2100; *kazy*, *ramnit*, and *outbrowse* share G2087. This demonstrates that a family can exhibit more than one type of behavior, and that some of these behaviors are shared by different families.

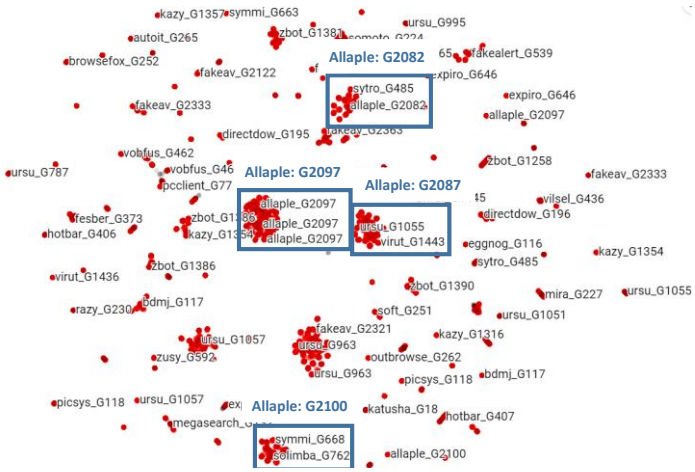

Fig. 9. 2D embedding of all profile representations from training set

VIII. CONCLUSION

In this study, we propose representing a malware sample using one or more embedded characteristics, matching behavior patterns learned from a family, which goes beyond traditional methods which predict only whether an unknown sample is malicious or classify its family. We propose a novel neural network framework for learning malware representations which utilizes BERT and Sent2Vec to extract the properties of a single API call as well as consecutive API calls, uses GRU and self-attention to reflect dependencies among API calls, and also uses a filter to determine significant API calls. We examine the effects of each component of the proposed model and show that the combination of all components, in particular full API call embeddings and ordinal information encoding, yields the best performance. Moreover, in an evaluation of family classification, 97.65% of unseen malicious execution traces were successfully classified on the basis of embedded characteristics that match previously collected families.

REFERENCES

[1] M. G. Schultz, E. Eskin, F. Zadok, and S. J. Stolfo, "Data mining methods for detection of new malicious executables," *In IEEE Symposium on Security and Privacy*. pp. 38-49, 2001.

[2] H. H. Feng, J. T. Giffin, Y. Huang, S. Jha, W. Lee, and B. P. Miller, "Formalizing sensitivity in static analysis for intrusion detection," *In Security and Privacy*, pp. 194-208, 2004.

[3] T. Abou-Assaleh, N. Cercone, V. Keselj, and R. Sweidan, "N-gram based detection of new malicious code," *Int. Comput. Softw. Appl.*, vol. 2, no. 1, pp. 41–42, 2004.

[4] A. Moser, C. Kruegel, and E. Kirda, "Limits of static analysis for malware detection," *In IEEE Annual Computer Security Applications Conference*, pp. 421-430, 2007.

[5] J. Saxe and K. Berlin, "Deep neural network based malware detection using two dimensional binary program features," *in Int. Conf. Malicious Unwanted Softw. (MALWARE)*, pp. 11–20, 2015.

[6] Y. Ye, T. Li, D. Adjeroh, and S. S. Iyengar, "A survey on malware detection using data mining techniques," *ACM Comput. Surv.*, vol. 50, no. 3, pp. 1–40, 2017.

[7] R. Agrawal, J. W. Stokes, M. Marinescu, and K. Selvaraj, "Neural sequential malware detection with parameters," *in IEEE International Conference on Acoustics, Speech and Signal Processing (ICASSP)*, pp. 2656-2660, 2018.

[8] R. Agrawal, J. W. Stokes, K. Selvaraj, and M. Marinescu, "Attention in recurrent neural networks for ransomware detection," *in IEEE International Conference on Acoustics, Speech and Signal Processing (ICASSP)*, pp. 3222-3226, 2019.

[9] M. Bailey, J. Oberheide, J. Andersen, Z. M. Mao, F. Jahanian, and J. Nazario, "Automated classification and analysis of internet malware," *in International Workshop on Recent Advances in Intrusion Detection*, pp. 178-197, 2007.

[10] A. Krizhevsky, I. Sutskever, and G. E. Hinton. "Imagenet classification with deep convolutional neural networks." *in Advances in Neural Information Processing Systems*, pp. 1097-1105, 2012.

[11] G. E. Dahl, J. W. Stokes, L. Deng, and D. Yu, "Large-scale malware classification using random projections and neural networks," *in Acoustics, Speech and Signal Processing (ICASSP)*, pp. 3422-3426, 2013.

[12] E. Gandotra, D. Bansal, and S. Sofat, "Malware analysis and classification: A survey," *Journal of Information Security*, vol. 5, pp. 56-64, 2014.

[13] O. E. David and N. S. Netanyahu, "DeepSign: Deep learning for automatic malware signature generation and classification," *in Int. Joint Conf. Neural Netw. (IJCNN)*, pp. 1–8, 2015.

[14] B. Athiwaratkun, and J. W. Stokes. "Malware classification with LSTM and GRU language models and a character-level CNN." *in IEEE International Conference on Acoustics, Speech and Signal Processing (ICASSP)*, pp. 2482-2486, 2017.

[15] M. Christodorescu, and J. Somesh, "Static analysis of executables to detect malicious patterns," *Wisconsin univ-madison dept of computer sciences*, 2006.

[16] M. Sebastián, R. Rivera, P. Kotzias, and J. Caballero. "Avclass: A tool for massive malware labeling." *In International Symposium on Research in Attacks, Intrusions, and Defenses*, pp. 230-253, 2016.

[17] W. J. Chiu. "Automated malware family signature generation based on runtime API call sequence," M.S. thesis, Information Management, National Taiwan University, Taiwan, 2017.

[18] M. Egele, T. Scholte, E. Kirda, and C. Kruegel, "A survey on automated dynamic malware-analysis techniques and tools," *In ACM computing surveys (CSUR)*, vol. 44, no. 2, p. 6, 2012.

[19] J. Devlin, M. W. Chang, K. Lee, and K. Toutanova, "Bert: pre-training of deep bidirectional transformers for language understanding," *arXiv preprint arXiv:1810.04805*, 2018.

[20] M. Pagliardini, P. Gupta, and M. Jaggi, "Unsupervised learning of sentence embeddings using compositional n-gram features," *arXiv preprint arXiv:1703.02507*, 2017.

[21] K. Cho, B. van Merrienboer, D. Bahdanau, and Y. Bengio. "On the properties of neural machine translation: encoder-decoder approaches," *arXiv preprint arXiv:1409.1259*, 2014.

[22] A. Vaswani, N. Shazeer, N. Parmar, J. Uszkoreit, L. Jones, A. N. Gomez, I. Polosukhin, "Attention is all you need," *in Advances in neural information processing systems*, pp. 5998-6008, 2017.

[23] H. Chen, D. Dean, and D. A. Wagner, "Model checking one million lines of C code," *in NDSS Symposium*, pp. 171-185, 2004.

[24] I. Santos, F. Brezo, X. Ugarte-Pedrero, and P. G. Bringas. "Opcode sequences as representation of executables for data-mining-based unknown malware detection," *Information Sciences*, 231, pp. 64-82, 2013.

[25] H. Hashem, A. Azmoodeh, A. Hamzeh, and S. Hashemi, "Graph embedding as a new approach for unknown malware detection," *Journal of Computer Virology and Hacking Techniques*, vol. 13, no. 3 pp. 153-166, 2017.

[26] D. Ucci, L. Aniello, and R. Baldoni, "Survey on the usage of machine learning techniques for malware analysis," *arXiv preprint arXiv:1710.08189*, 2017

[27] J. Kolter, and M. Maloof, "Learning to detect malicious executables in the wild," *in ACM SIGKDD International Conference on Knowledge Discovery and Data Mining*, pp. 470-478, 2004.

[28] R. Tian, M. R. Islam, L. Batten, and S. Versteeg, "Differentiating malware from cleanwares using behavioral analysis," *in International Conference on Malicious and Unwanted Software (Malware)*, pp. 23-30, 2010.

[29] S. W. Hsiao, Y. N. Chen, Y. S. Sun, and M. C. Chen, "A cooperative botnet profiling and detection in virtualized environment," *in IEEE Conference on Communications and Network Security (CNS)*, pp. 154-162, 2013.

[30] S. W. Hsiao, Y. S. Sun, and M. C. Chen, "Virtual machine introspection based malware behavior profiling and family grouping," *arXiv preprint arXiv:1705.01697*, 2017.

[31] S. B. Needleman and C. D. Wunsch, "A general method applicable to the search for similarities in the amino acid sequence of two proteins," *Journal of molecular biology*, vol. 48, no. 3, pp. 443-453, 1970.

[32] Y. T. Huang, Y. Y. Chen, C. C. Yang, Y. S. Sun, S. W. Hsiao, and M. C. Chen. "Tagging malware intentions by using attention-based sequence-to-sequence neural network." In *Australasian Conference on Information Security and Privacy*, pp. 660-668, 2019.

[33] D. P. Kingma, and J. Ba, "Adam: A method for stochastic optimization," *arXiv preprint arXiv:1412.6980*, 2014.

[34] Y. Bengio, P. Simard, and P. Frasconi, "Learning long-term dependencies with gradient descent is difficult," in *IEEE Transactions on Neural Networks*, vol. 5, no. 2, pp. 157–166, 1994.

[35] R. Caruana, S. Lawrence, and C. L. Giles, "Overfitting in neural nets: Backpropagation, conjugate gradient, and early stopping." in *Advances in neural information processing systems*, pp. 402-408, 2001.

[36] L. McInnes, J. Healy, and J. Melville. "Umap: Uniform manifold approximation and projection for dimension reduction." *arXiv preprint arXiv:1802.03426*, 2018.